Food Chemistry: X 22 (2024) 101506

Contents lists available at ScienceDirect

Food Chemistry: X

journal homepage: www.sciencedirect.com/journal/food-chemistry-x

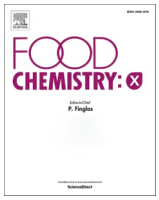

Encapsulation of zingerone by self-assembling peptides derived from fish viscera: Characterization, interaction and effects on colon epithelial cells

Sirong Huang [a,b,1], Xintong Yao [c,1], Boya Cao [a,b], Na Zhang [d], Olugbenga P. Soladoye [e], Yuhao Zhang [a,b], Yu Fu [a,b,*]

[a] College of Food Science, Southwest University, Chongqing 400715, China
[b] Chongqing Key Laboratory of Speciality Food Co-Built by Sichuan and Chongqing, Chongqing 400715, China
[c] Department of Hematology, The First Affiliated Hospital of Army Medical University, Chongqing, 400038, China
[d] Key Laboratory of Food Science and Engineering of Heilongjiang Province, College of Food Engineering, Harbin University of Commerce, Harbin 150076, China
[e] Agriculture and Agri-Food Canada, Government of Canada, Lacombe Research and Development Centre, 6000 C&E Trail, Lacombe, Alberta T4L 1W1, Canada

ARTICLE INFO

Keywords:
Peptides
Fish viscera
Zingerone
Encapsulation
Self-assembly
Interaction

ABSTRACT

The purpose of the present work was to encapsulate zingerone (a bioactive compound from ginger) by self-assembling peptides derived from fish viscera. The encapsulation conditions were investigated and the structure of fish peptides-zingerone complex was characterized. The interaction between zingerone and fish peptides was investigated using fluorescence spectroscopy. Further research was performed on the *in vitro* release of zingerone and fish peptide-zingerone as well as their antiproliferative effects on colon epithelial Caco-2 cells. The results demonstrated that zingerone can be successfully encapsulated by self-assembling peptides derived from fish viscera with high encapsulation efficiency and loading capacity. Furthermore, transmission electron microscope and confocal laser scanning microscope observations revealed the successful encapsulation of zingerone by fish viscera peptides. In addition, *in vitro* release and antiproliferative activity against Caco-2 cells can be significantly increased by encapsulating zingerone *via* peptide self-assembly. The current study advances knowledge of encapsulation of bioactive compounds through peptide self-assembly.

1. Introduction

Molecular self-assembly is a spontaneous process that utilizes non-covalent interactions to fabricate biopolymers into stable nanostructures (Li, Lu, Zhang, Hu, & Li, 2022). Peptides are amphiphilic compounds with both hydrophobic and hydrophilic moieties, which can satisfy the premise for self-assembly (Chen, Cai, Cheng, & Wang, 2022). Among different raw materials, self-assembly by peptides can be achieved through a relatively simple processing approach (Chen et al., 2022; Chen, Cai, et al., 2022). Therefore, when using peptide as a carrier, peptide self-assembly can be employed to generate an emulsion system or encapsulate bioactive compounds (Vahedifar & Wu, 2022). In recent years, application of food protein-derived peptides in encapsulation systems has attracted extensive attention. For instance, Zhang et al. (2018) have prepared soybean peptide-based nanoparticles (SPN) using ultrasound treatment. The SPN formed by self-assembly can stabilize the O/W emulsion. Li and Yao (2020) have demonstrated that zein peptides prepared by Alcalase can encapsulate curcumin by peptide self-assembly in an aqueous solution to obtain a peptide-curcumin complex with a high encapsulation efficiency. Moreover, zein peptides can effectively improve the solubility of curcumin and prevent curcumin from degradation based on the results of storage stability. In addition, the bioavailability of curcumin in the digestive solution was as high as 75%, and the peptide-curcumin complex showed a potent antioxidant effect after oral administration based on the rat model *in vivo* (Li & Yao, 2020). Recently, our group has revealed that encapsulation of β-carotene can be achieved by self-assembly of rapeseed meal-derived peptides. The water solubility of β-carotene was significantly improved, and the stability under high temperatures and UV irradiation was also enhanced (Lan et al., 2021). Overall, protein hydrolysates/peptides obtained by enzymatic hydrolysis of food proteins can not only stabilize the emulsion, but also improve the solubility, prevent degradation and elevate the bioavailability of bioactive compounds by self-assembly of nanoparticles (Chen, Cai, et al., 2022; Chen, Chen, et al., 2022). In

* Corresponding author at: College of Food Science, Southwest University, Chongqing 400715, China.
E-mail address: fuy987@swu.edu.cn (Y. Fu).
[1] These authors contributed equally to this work.

https://doi.org/10.1016/j.fochx.2024.101506
Received 26 August 2023; Received in revised form 7 May 2024; Accepted 22 May 2024
Available online 24 May 2024

addition, it has been shown that encapsulation of hydrophobic bioactive compounds by peptide self-assembly can increase their solubility, stability and bioavailability (Chen et al., 2021; Yang et al., 2022).

Ginger (*Zingiber officinale* Roscoe) is a herbaceous plant that is commonly used as a spice around the globe (Gao et al., 2022). Zingerone (4- (4-hydroxy-3-methoxyphenyl)-2-butanone), a major phytochemical compound in ginger extract (9.25%), has been reported to exhibit antioxidant, anti-inflammatory, anti-atherosclerotic and anti-cancer activities (Amin et al., 2021; Elshopakey et al., 2022; Rashid et al., 2021; Wali et al., 2020). However, due to its susceptibility to oxygen, light, and high temperatures, zingerone is prone to degradation, which could impair its bioactivity and limit its use as a bioactive ingredient in food products (Su et al., 2019). As a result, encapsulating zingerone through peptide self-assembly can be a feasible strategy. It has been shown that the interaction between proteins and polyphenols can somewhat exert an impact on the biological function of polyphenols (Fu, Liu, & Soladoye, 2021). Even though several existing studies have mainly emphasized the interaction between proteins and polyphenols (Ma & Zhao, 2019), there is a dearth of studies focusing on protein hydrolysates/peptides.

During fish processing, a large amount of fish co-products (*e.g.* viscera, head, skin and bones, etc) can be generated, which are abundant in protein (Luo, Yao, Soladoye, Zhang, & Fu, 2021). Fish viscera possess high contents of proteins and lipids, so high-efficiency utilization of fish viscera can be economically and environmentally beneficial to fish processing industry (Villamil, Váquiro, & Solanilla, 2017). Enzymatic hydrolysis is a feasible strategy for the conversion of protein into soluble peptides. Such peptides can be used for encapsulation of certain bioactive compounds and improve their stability as well as bioavailability. Moreover, it would be valuable to understand the interaction between fish viscera-derived peptides and zingerone for the subsequent bioactivity. Therefore, the aims of the current study were to encapsulate zingerone by self-assembling peptides from fish viscera and explore the interaction between peptides and zingerone. In addition, the *in vitro* release and antiproliferative effect of peptide-zingerone complex on human intestinal Caco-2 epithelial cells was investigated.

2. Materials and methods

2.1. Materials

The fish viscera powder from grass carp (protein content, 27.5%) was kindly donated from Haohu Fishery Co., Ltd. (Chongqing, China). Alcalase and Tris, Dulbecco's Modified Eagle Medium (DMEM), fetal bovine serum (FBS) and 3-(4,5-Dimethylthiazol-2-yl)-2,5-diphenyltetrazolium bromide (MTT) were obtained from Beijing Solario Science and Technology Co., Ltd. (Beijing, China). Zingerone (purity≥98%), 1-anilino-8-naphthalene sulfonic acid (ANS) and *o*-phthaldialdehyde (OPA) were purchased from Aladdin Biochemical Technology Co., Ltd. (Shanghai, China). Hydrochloric acid and sodium hydroxide were bought from Chron Chemicals Co., Ltd. (Chengdu, China). Anhydrous ethanol was purchased from Chongqing Chuandong Chemical Co., Ltd. (Chongqing, China). The other reagents used in this study were of analytical grade.

2.2. Enzymatic hydrolysis of fish viscera protein

Enzymatic hydrolysis of fish viscera protein was conducted according to the following conditions. The pH of fish viscera protein solution (10%, *w/v*) was adjusted to 8.5 with 2.0 mol/L NaOH, and the temperature was adjusted to 55 °C. Enzymatic hydrolysis was initiated by adding 1% Alcalase (enzyme-substrate ratio, *w*/w) at the speeds of 300 rpm. At each time point (30, 60, 90, 120, 150 and 180 min), protein hydrolysates were withdrawn and transferred into boiling water to inactive the enzyme for 15 min, followed by further cooling to room temperature (25 °C). Subsequently, the resultant protein hydrolysates (supernatant) were recovered by centrifugation (6000*g*) for 15 min at 25 °C, freeze-dried and stored at −20 °C until further analysis.

2.3. Determination of degree of hydrolysis (DH)

The DH was measured by OPA method according to previous methods (Fu et al., 2020). In brief, 1.2 mL of OPA reagent was added to the sample solution of 10 μL. The OPA reagent was further agitated with a magnetic stirrer for an additional hour, while being kept in the dark. After incubating the sample solution for 10 min at 25 °C, the absorbance of solution at 340 nm was measured. The concentrations of free amino group in the samples were calculated using the standard curve of Leu standards. With the aid of the following formula, DH was subsequently determined.

$$\mathrm{DH}\ (\%) = \frac{[\mathrm{NH2}] \times \mathrm{V1}}{[\mathrm{NH2}]1 \times \mathrm{V2}} \times 100\%$$

where $[NH_2]$ and $[NH_2]_1$ are the corresponding contents of free amino group in protein hydrolysate and fish viscera solution, while V_1 and V_2 are the volume of protein hydrolysate and fish viscera solution, respectively.

2.4. Determination of peptide size distribution

The peptide size distributions of fish viscera protein hydrolysates were assayed using high-performance liquid chromatography (Ultimate 3000, Thermo Fisher, Waltham, Massachusetts, USA) equipped with a size exclusion column (Phenomenex BioSep™ SEC-S2000 column, 300 mm × 4.6 mm) according to our previous method (Fu, Liu, Hansen, Bredie, and Lametsch (2018). The employed molecular weight standards included cytochrome C (12.5 kDa), Gly-Gly-Tyr-Arg (451 Da), trasylol (6.51 kDa), and human serum albumin (66 kDa).

2.5. Surface hydrophobicity (S_0)

The surface hydrophobicity of samples was assessed as per the method of Lan et al. (2021). ANS, the fluorescent probe, was employed in this method, and the relative fluorescence intensity was determined at the excitation wavelength of 390 nm and the emission wavelength of 470 nm with the aid of F-2500 fluorescence spectrophotometer (Hitachi, Japan). The relative fluorescence intensity was plotted *versus* each concentration of the samples used, and S_0 was calculated from the initial slope of curve.

2.6. Preparation of fish peptide–zingerone complex

The stock solutions of fish viscera-derived peptides (20 mg/mL) and zingerone (100 μM) were prepared using phosphate buffered saline (0.1 mol/L, pH 7.0). The stock zingerone solutions were added to fish viscera peptide solution to obtain serial concentrations of zingerone, followed by magnetic stirring for a period of time (0−12*h*). The final concentration of fish viscera peptides was fixed at 2 mg/mL, and the concentration of zingerone varied from 0 to 20 μmol/L.

2.7. Encapsulation efficiency (EE) and loading capacity (LC)

EE is the ratio of the initial amount of bioactive compound to the amount of bioactive compound that has been encapsulated in the core of carrier. The measurement of EE was performed according to the previously reported method described by Ge et al. (2021). The high performance liquid chromatography (HPLC) system (Ultimate 3000, Thermo Fisher Scientific Co., Ltd., USA) equipped with Agilent ZORBAX SB-C18 (4.6 × 150 mm, 5 μm) was employed to quantify the content of zingerone. The chromatographic conditions were listed as follows: mobile phase, aqueous methanol solutions (70%, *v*/v); column temperature,

37 °C; flow rate, 1.0 mL/min; detection wavelength, 280 nm. The amount of free zingerone was quantified so that EE and LC were calculated through the following calculation formula.

$$EE(\%) = \frac{\text{m(Encapsulated zingerone)}}{\text{m(Total zingerone)}} \times 100\%$$

$$LC(\%) = \frac{\text{m(Encapsulated zingerone)}}{\text{m(Peptide} - \text{zingerone complex)}} \times 100\%$$

m(Encapsulated zingerone) is the amount of encapsulated zingerone, m(Total zingerone) is the total content of zingerone, and m(Peptide-zingerone complex) is the total mass of peptide-zingerone complex.

2.8. Transmission electron microscope (TEM)

The microstructure and morphology of fish peptide-zingerone complex were investigated by TEM according to our previous method (Lan et al., 2021). A copper grid coated with a carbon support film was used to hold a droplet of the sample solution, which was allowed to sit for 5 min before removing the excessive solution with filter paper. The grid was further treated with a droplet of phosphotungstic acid (1%, *w/v*), left for another 5 min, and the surplus solution was removed as well. Subsequently, the material was examined *via* TEM (JEM-1200EX, JEOL Ltd., Tokyo, Japan) after being dried at an acceleration voltage of 100 kV.

2.9. Confocal laser scanning microscopy (CLSM)

The morphological characteristics of the resultant fish peptide-zingerone complex were observed using a Zeiss CLSM 800 confocal microscope (Carl Zeiss GmbH, Jena, Germany) (Lan et al., 2021). For this purpose, a 40 × objective lens and a 10 × eyepiece lens were employed. Furthermore, Nile Blue (0.1%, w/v) dissolved in water and Nile Red (0.1%, w/v) dissolved in isopropanol were adopted to stain the fish peptides and zingerone, respectively.

2.10. Fluorescence spectrometry assay

The F-4500 fluorescence spectrophotometer (Hitachi, Kyoto, Japan) was used to examine the fluorescence spectra of the complex of fish viscera peptides and zingerone according to Ma and Zhao (2019). The mixture solutions were put into quartz cuvettes and immediately scanned following 30-min incubation period at each of three different temperatures (298, 308, and 318 K). At 280 nm, the excitation wavelength was set, while the scan of emission was implemented between 290 and 400 nm. The slit widths of excitation and emission were both set to 5 nm.

Additional investigations were conducted to elucidate the mechanism of fluorescence quenching. Dynamic quenching and static quenching are two basic methods that can be classified as fluorescence quenching processes. The fluorescence quenching mechanism between peptides and zingerone was examined using the Stern-Volmer equation (Eq. 1).

$$F0/F = 1 + Ksv \cdot Q = Kq \cdot \delta 0 \cdot Q \quad (1)$$

Fish viscera peptides with or without zingerone are represented by the relative fluorescence intensities F and F_0 in Eq. 1. The quenching concentration of zingerone is Q, and K_{sv} stands for the Stern-Volmer quenching rate constant. The average lifetime of biomacromolecules is roughly 10^{-8} s, and K_q is the quenching rate constant. And δ_0 is the average lifetime of fluorescents in the absence of a quenching agent. The main source of fluorescence quenching when K_q is higher than the maximal diffusion collision quenching constant 2×10^{10} L/(mol·s) is static quenching.

Additionally, the apparent binding constant and the number of binding sites were computed. The double logarithm equation can be used to determine the apparent binding constant (K_a) and number of binding sites (n) for the interaction between peptides and zingerone in terms of static quenching (Eq. 2).

$$lg\,[(F0 - F)/F\,] = lg\,Ka + n \cdot lg\,Q \quad (2)$$

In Eq. 2, fish peptides with and without zingerone are represented by the relative fluorescence intensities (F and F_0). Q represents the amount of zingerone.

Eq. 3 employs the Van't Hoff equation to calculate the changes in enthalpy and entropy (ΔH and ΔS) and the Gibbs-Helmholtz equation to estimate the change in free energy (ΔG) in order to further identify the thermodynamic parameters involved in the interaction between fish viscera peptides and zingerone (Eq. 4).

$$ln\,Ka = -\Delta H/(R \cdot T) + \Delta S/R \quad (3)$$

$$\Delta G = \Delta H - T \cdot \Delta S \quad (4)$$

In Eq. 3 and 4, R represents the constant (8.314 $J \cdot mol^{-1} \cdot K^{-1}$), and T represents the absolute temperature.

2.11. In vitro release study

The *in vitro* release of zingerone and fish peptide-zingerone complex was evaluated based on the dialysis diffusion method (Yu, Yuan, Li, Schwendeman, & Schwendeman, 2019). Specifically, zingerone and fish peptide-zingerone complex were added to two media, namely double-distilled water and 0.1 mol/L phosphate buffered saline (pH 6.8), followed by further agitation for an additional 0.1 to 24 h at the rotation speed of 100 rpm. At each time interval (0.1, 0.2, 0.5, 1, 2, 3, 6, and 24 h), a sample of 1 mL was withdrawn and immediately replaced with an equal volume of double-distilled water or phosphate buffered saline at 37 °C. The content of zingerone was quantified by the HPLC method as described in Section 2.7.

2.12. In vitro antiproliferation study

Caco-2 cells, a cell line originating from human colon carcinoma, were grown in Dulbecco's Modified Eagle Medium (DMEM) with 10% fetal bovine serum, 100 μg/mL of penicillin and streptomycin and 1% non-essential amino acids. The cells were incubated in a fully humidified atmosphere at the temperature of 37 °C under a humidified atmosphere of 5% carbon dioxide/ 95% air. The media used for cell culture was replaced every other day.

To investigate the antiproliferative effects of zingerone and peptide-zingerone complex on Caco-2 cells, the MTT assay (Fu & Zhao, 2015) was employed. Briefly, Caco-2 cells were seeded onto a 96-well culture plate and treated with varying concentrations (2, 10, 50, 100, 200 μg/mL) of zingerone or peptide-zingerone complex at 37 °C in 5% CO_2 for 24 or 48 h. Afterward, each well received 20 μL of MTT (5 mg/mL) and was further incubated for 4 h. Thereafter, 150 μL of dimethyl sulfoxide (DMSO) was added to dissolve the formazan crystals. Finally, the absorbance was measured at 490 nm using the BioTek Synergy HT microplate reader (BioTek Instruments Inc., Vermont, USA).

$$\text{Cell viability}(\%) = \frac{\text{Absorbance (sample)} - \text{Absorbance (blank)}}{\text{Absorbance (control)} - \text{Absorbance (blank)}} \times 100\%$$

2.13. Statistical analysis

Data were presented as the mean ± standard deviation for each experiment, which was carried out in triplicate. With the aid of statistical analysis program SPSS 21.0, the results were statistically evaluated using a one-way analysis of variance (ANOVA) with a significance level ($P < 0.05$) and Duncan multiple range post-hoc tests were used.

3. Results and discussion

3.1. Degree of hydrolysis of fish viscera

The DH curve of fish viscera is depicted in Fig. 1a, which indicates that DH gradually elevated with the prolonged hydrolysis time. The hydrolysis rate exhibited a notable deceleration with an increase in hydrolysis time, as evidenced by the slope of DH. Following a 150-min enzymatic hydrolysis, the DH in the fish viscera protein hydrolysates was determined to be 17.9%. Alcalase, a highly effective endoprotease, has been proven to be useful for producing high DH *via* enzymatic hydrolysis of dietary proteins. The observations pertaining to alterations in the enzymatic hydrolysis rate were in agreement with those reported in a previous study (Ketnawa, Benjakul, Martínez-Alvarez, & Rawdkuen, 2017).

As can be observed in Fig. 1b, the percentage of fish viscera peptides with molecular weight of >10 kDa was gradually reduced along with the enzymatic hydrolysis, and the percentage of peptide fraction (<3 kDa) also increased significantly with the extended hydrolysis time. The outcomes of the peptide size distribution analysis were consistent with the DH values, wherein a higher DH correlated with the generation of a greater quantity of low-molecular-weight peptides.

Fig. 1c depicts that as the hydrolysis time reached 180 min, the S_0 values of fish viscera peptides gradually decreased from 760.1 to 405.5. Proteins underwent a gradual transformation into hydrophilic-shaped peptides during continuous enzymatic hydrolysis, subsequently enhancing protein solubility. Given that the predominant portion of encapsulated bioactive compounds, *e.g.* zingerone, is hydrophobic, the use of a carrier (in this study, fish viscera peptides) becomes imperative. A previous study has revealed that hydrophobic interactions have been identified as one of the primary driving mechanisms underlying the self-assembly process of amphiphilic peptides (Zhao et al., 2018).

Taken together, it has been shown that peptides with both hydrophobic and hydrophilic properties tend to exhibit an enhanced self-assembly capacity, while peptides with excessively long or short chains do not contribute favorably to the process of peptide self-assembly (Chen, Cai, et al., 2022; Chen, Chen, et al., 2022; Vahedifar & Wu, 2022). Based on the present results from peptide size distribution and hydrophobicity, enzymatic hydrolysis for 120 min was selected as the optimal condition for the subsequent encapsulation of zingerone by peptide self-assembly.

3.2. Optimization of encapsulation conditions

3.2.1. Effect of hydrolysis time on encapsulation capacity of fish viscera peptides

The effect of hydrolysis time on the encapsulation capacity was investigated. Fig. 2a illustrates the outcomes of the encapsulation of zingerone by fish viscera peptides subjected to varying hydrolysis times. Zingerone was encapsulated by fish viscera peptides as the hydrolysis time extended, resulting in a gradual and ultimately stabilized increase in encapsulation efficiency, particularly evident after 120 min. At 120 min, the maximal EE value (89.1%) was attained. Presumably, the favorable hydrophobic characteristics of peptides at this time facilitated the encapsulation of zingerone by self-assembled peptides, as indicated by the marginal decrease ($P > 0.05$) in the EE value observed with the extension of hydrolysis time to 180 min. Considering the efficiency in reaction time and energy conservation, a hydrolysis duration of 120 min was selected for the subsequent investigation into encapsulation.

3.2.2. Effect of encapsulation time on encapsulation capacity of fish viscera peptides

As shown in Fig. 2b, the impacts of encapsulation time on the encapsulation capacity of peptides were studied. With the extension of encapsulation time, the value EE significantly increased in the initial 3 h ($P < 0.05$). When the encapsulation time reached 3 h, EE was the highest (85.1%). However, with the extended encapsulation time, EE decreased slightly ($P > 0.05$). This phenomenon could be attributed to the instability of the encapsulation structure induced by excessive stirring (Zhao, Guo, Ding, Ye, & Liu, 2020), which led to the further release of zingerone in the encapsulation system and resulted in the relatively low EE. Therefore, the optimal encapsulation time for subsequent experiments was fixed at 3 h.

3.2.3. Effect of zingerone/peptides ratios on encapsulation capacity

Fig. 2c illustrates that EE of peptides remained high (> 80%), when the mass ratio of zingerone to peptides ranged from 1:3 to 1:6 (*w*/w). Nevertheless, when the ratio fell below 1:3 (w/w), the LC exhibited a notable decline, implying that the quantity of zingerone might have surpassed the loading capacity of the peptides. At the ratio of 1:1 (w/w), both EE and LC exhibited relatively low values. This outcome is attributed to the excessive addition of zingerone, leading to the aggregation of the encapsulation complex and subsequent precipitation during the magnetic stirring process, resulting in decreased EE and LC (Akbari & Wu, 2016). Therefore, the optimal mass ratio of zingerone to peptide was set at 1:3 (w/w). Collectively, according to the results of factor optimization, 120-min hydrolysis was employed for the follow-up analysis. The optimal encapsulation time was fixed at 3 h, and the ideal mass ratio of zingerone to peptide was fixed at the ratio of 1:3 (w/w). Consequently, the self-assembly morphology of the resultant products was further analyzed using the optimized conditions, which was reasonable according to the recently reported literature (Lan et al., 2021; Yu et al., 2022).

3.3. Morphological analysis

3.3.1. CLSM

CLSM is able to characterize the microstructure of the encapsulation

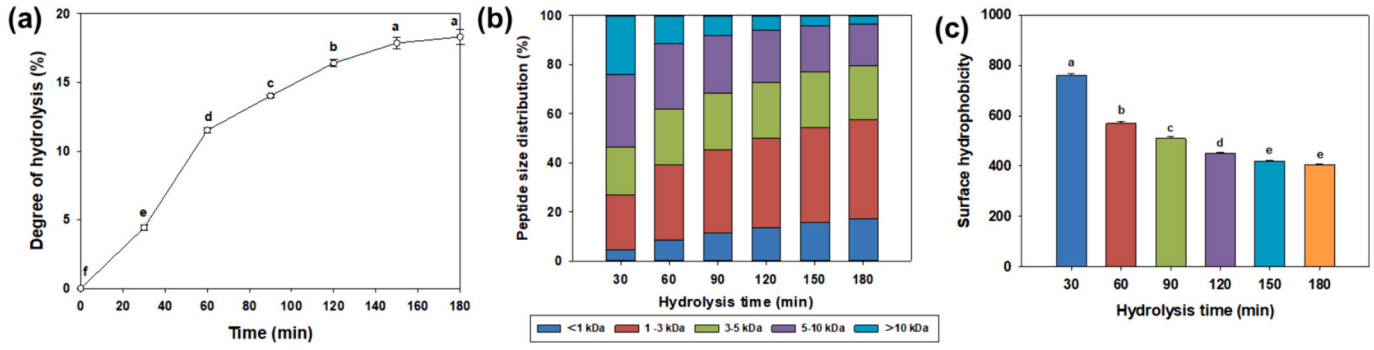

Fig. 1. Hydrolysis curve of peptides from fish by-products (a); peptide size distribution (b); S_0 of peptides at different hydrolysis times (30, 60, 90, 120, 150, 180 min) (c). Different letters indicate that there is a statistically significant difference between groups ($P < 0.05$).

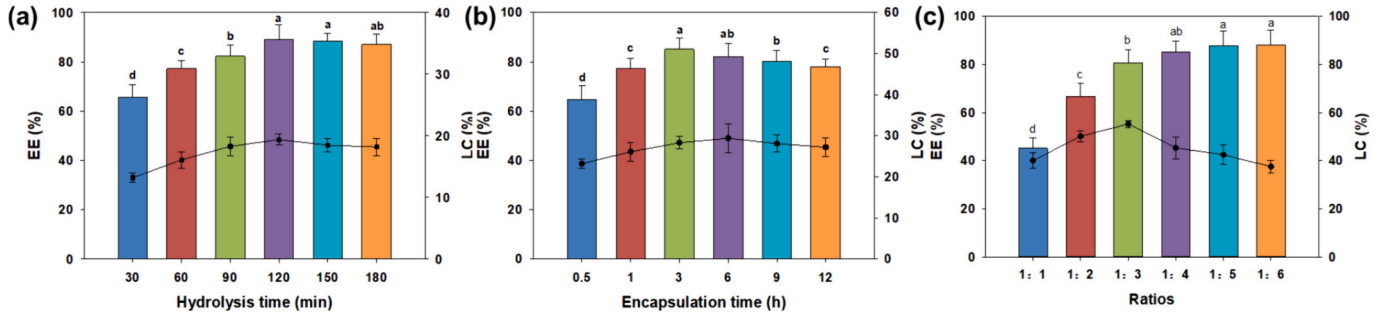

Fig. 2. Impacts of different hydrolysis times (a), different encapsulation times (b) and different ratios (c) on encapsulation efficiency (EE) and loading capacity (LC). Different letters indicate that there is a statistically significant difference between groups ($P < 0.05$).

complex through fluorescence observations (Du et al., 2019), which can be used to confirm the successful encapsulation of zingerone by fish viscera peptides. As shown in Fig. 3a & b, fish viscera peptides stained with Nile blue were red, while zingerone stained with Nile red was green (left). When the images (left and middle) are combined, if the image exhibits an orange hue, it indicates the formation of the peptide-zingerone complex (Liu, Wang, McClements, & Zou, 2018). As can be seen in Fig. 3c, the complex of fish viscera peptide and zingerone was successfully prepared when a predominant portion of the visual field in the image transitioned to orange particles. It is noteworthy that while the resulting complex solution exhibited a predominantly uniform appearance, the sizes of the particles varied significantly. The encapsulation complex in the aqueous solution manifested diverse sizes due to the distinct molecular weights and polarities within the peptide mixture system, which was in agreement with a previous study by Du et al. (2019).

3.3.2. TEM

The disparities in the shape and size of the samples before and after encapsulation were investigated. The freshly synthesized fish viscera peptides and the peptides-zingerone complex were subsequently investigated using TEM to provide a more detailed observation of the microscopic morphology of the materials. It is evident that encapsulation of zingerone resulted in increased particle size of the peptide-zingerone complex (Fig. 4). According to a previously reported study (Sotelo-Boyás, Correa-Pacheco, Bautista-Baños, & Corona-Rangel, 2017), the larger nanoparticle size observed implied the successful encapsulation of bioactive compounds, specifically zingerone in the present study, underscoring the influence of the encapsulated substance on particle size. The morphology of the encapsulation complex is also non-uniform, displaying a variety of shapes and degrees of aggregation, as depicted in the TEM images (Fig. 4). This may be attributed to the incorporation of peptides with different molecular weights and diverse amphiphilic properties into the peptide solution, contributing to the alterations in the structure of encapsulation complex (Lan et al., 2021). Based on the aforementioned findings, it can be inferred that the amphiphilic peptides produced by enzymatic hydrolysis with Alcalase could self-assemble and encapsulate zingerone in an aqueous environment to generate a peptide-zingerone complex (Kim, Thévenot, Ibarboure, Lecommandoux, & Chaikof, 2010).

3.4. Fluorescence spectroscopy

3.4.1. Fluorescence quenching mechanism analysis

The fluorescence spectra of fish viscera peptides containing various concentrations of zingerone at 298 K, 308 K and 318 K are illustrated in Fig. 5. It is evident that the fluorescence intensity of fish viscera peptides significantly decreased with increasing concentrations of zingerone, indicating that the interaction with zingerone led to the quenching of the intrinsic fluorescence emitted by the peptides (Cao et al., 2021). Moreover, each concentration exhibited a marginal red shift of approximately 2 nm, suggesting a tendency for the peptide structure to become more open. Additionally, the diminished fluorescence intensity was attributed to increased intrinsic fluorescence quenching observed at elevated temperatures (Yin et al., 2021).

3.4.2. Binding parameter analysis

The quenching constants, binding constants, and thermodynamic parameters are presented in **Table S1** to illustrate the fluorescence quenching mechanism. The K_q values were higher than the maximal diffusion collision quenching constant value at different temperatures (298 K, 308 K, and 318 K), indicating that the primary quenching mechanism was static quenching based on the formation of fluorophore-quencher complexes (Yin et al., 2021). The K_a values of the complexes followed the order of 10^6 and decreased with rising temperatures, indicating a firm binding of zingerone to peptides (Wu et al., 2021).

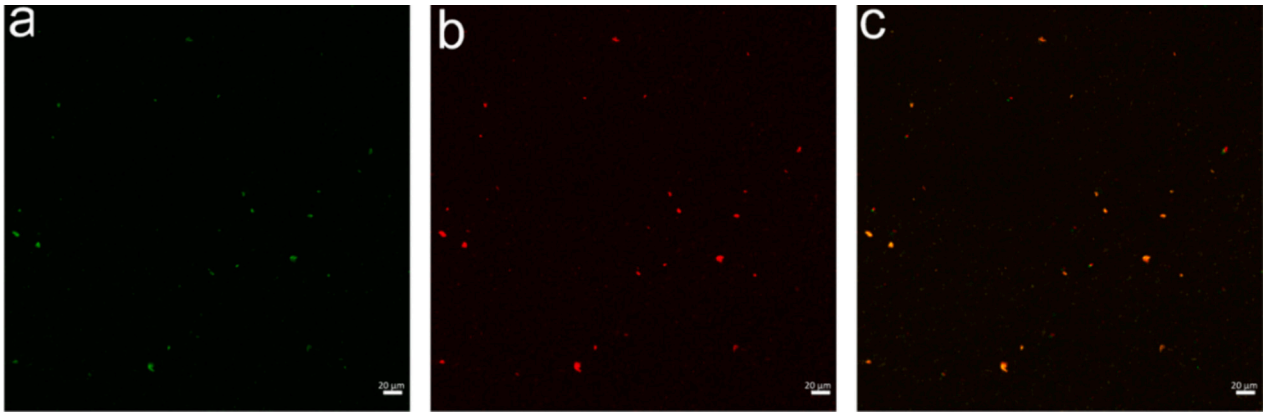

Fig. 3. CLSM images of zingerone (a), peptides (b) and peptides-zingerone complex (c).

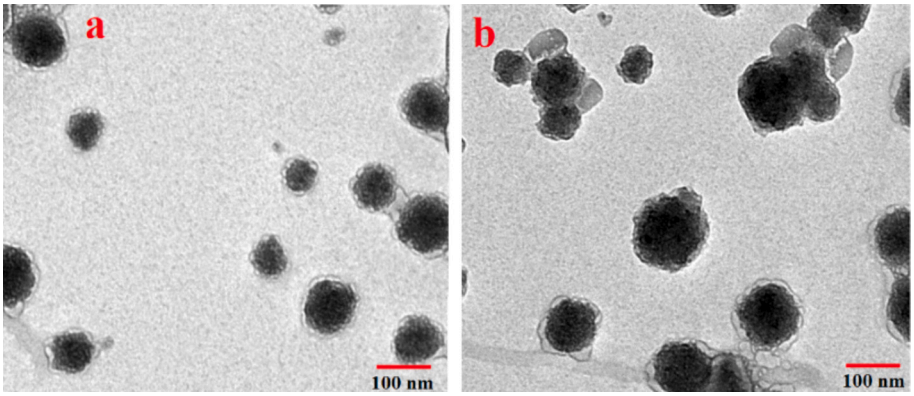

Fig. 4. TEM images of peptides (a) and peptides-zingerone complex (b).

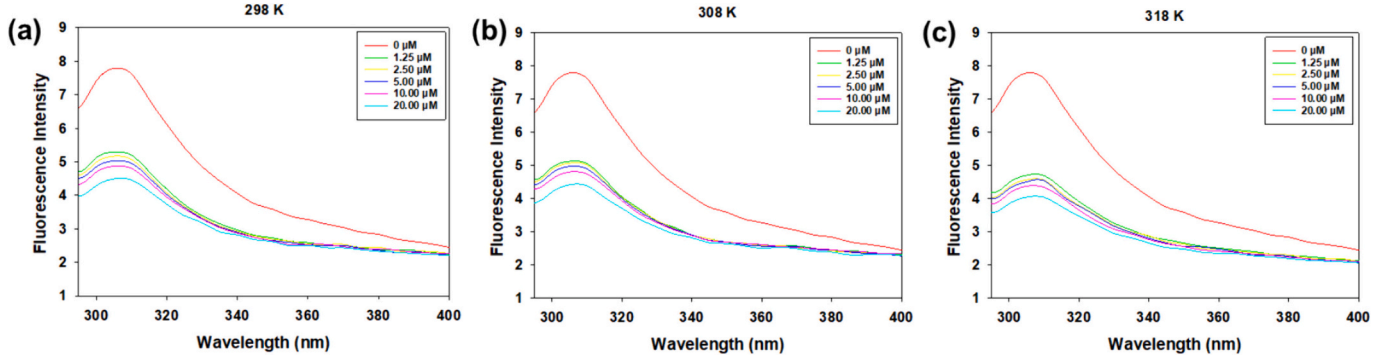

Fig. 5. Intrinsic fluorescence spectra of fish viscera peptides in the presence of 0, 1.25, 2.50, 5.00, 10.00, 20.00 μM at 298 K (a), 308 K (b) and 318 K (c).

Additionally, the n values were close to 1, indicating that there was approximately a single binding site for zingerone during the interaction with fish viscera peptides.

3.4.3. *Thermodynamic parameters and binding force analysis*

Thermodynamic parameters between fish viscera peptides and zingerone are also listed in **Table S1**, which are related to a noncovalent type of interaction. The negative ΔG values in the Van't Hoff equation revealed that the binding of fish peptides to zingerone was spontaneous (Wang et al., 2016). Moreover, $\Delta S < 0$ suggested that the predominant non-covalent interactions between fish peptides and zingerone were hydrophobic interaction and van der Waals force. As suggested by Dias et al. (2019), the negative ΔH value of fish viscera peptide-zingerone complex was an indicator of the exothermic interaction. This result could elucidate the variations observed in the association constant (K_a) values as a function of temperature.

3.5. *In vitro release study*

Through analysis of the released zingerone content from both free zingerone and the fish viscera peptide-zingerone complex in double distilled water and phosphate buffer solutions at distinct intervals, the *in vitro* release rate of zingerone was evaluated utilizing the HPLC method. The results showed that, in each medium, the cumulative release of the fish viscera peptide-zingerone complex was notably higher than that of free zingerone ($P < 0.05$), as depicted in Fig. 6. Following a 24-h *in vitro* release, the cumulative release rates of free zingerone in each medium were 30.6% (double distilled water) and 30.9% (phosphate buffer solution). In contrast, the cumulative release rates of the fish viscera peptide-zingerone complex were markedly higher, reaching 80.4% (double distilled water) and 80.9% (phosphate buffer solution). Hence, the findings of this study suggest that encapsulation could potentially augment the release of zingerone. This observation aligns with the

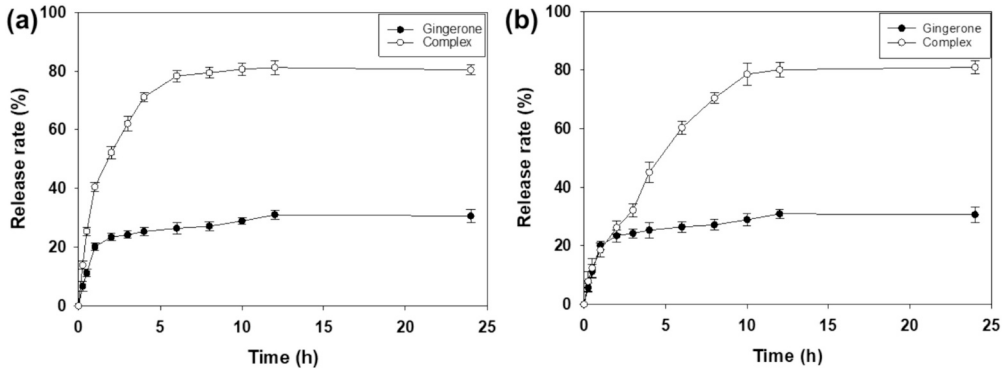

Fig. 6. *In vitro* release profiles of zingerone and peptides-zingerone complex in double-distilled water (a) and phosphate buffer solution (pH 6.8) (b).

notion that nano-encapsulation of bioactive compounds may enhance their *in vitro* release, as previously reported by Shishir, Xie, Sun, Zheng, and Chen (2018).

3.6. *In vitro* inhibitory activities towards Caco-2 cells

The MTT assay was employed to assess the *in vitro* inhibitory effects of both free zingerone and the fish peptide-zingerone complex on Caco-2 cells. Caco-2 cells treated with zingerone exhibited a diminishing trend in cell viability as concentrations increased during a 24-h treatment, as shown in **Fig. S1**. Notably, the proliferation of Caco-2 cells was observed to be inhibited in a dose-dependent manner in both the groups treated with free zingerone and the fish peptide-zingerone complex. The cell inhibitory activities of the fish viscera peptide-zingerone complex, as compared to free zingerone, exhibited a significant enhancement ($P < 0.05$), when zingerone was encapsulated by fish viscera peptides. In addition, the IC_{50} values of zingerone and fish peptide-zingerone complex were determined to be 10.62 μg/mL and 5.86 μg/mL, respectively. It is noteworthy that the IC_{50} value of the fish viscera peptide-zingerone complex was considerably lower than that of free zingerone. This discrepancy implies that the encapsulation system contributed to the heightened inhibitory potency in Caco-2 cells. Zingerone in the complex form can enter cells through carrier-mediated endocytosis due to the nano-size particle, whereas free zingerone can enter cells through passive diffusion (Rudke, Mazzutti, Andrade, Vitali, & Ferreira, 2019). In a similar vein, research so far has shown that encapsulation can enhance *in vitro* antiproliferative effects in addition to changing particle size (Kieler-Ferguson et al., 2017). Consequently, through peptide self-assembly, zingerone can be encapsulated to enhance its inhibitory effect against cancer cells *in vitro*, utilizing various cellular absorption pathways for both zingerone and the peptide-zingerone complex. However, the exact mechanism underlying the anti-proliferative effect of fish viscera peptide-zingerone complex has to be further studied.

4. Conclusion

The current work revealed that zingerone can be encapsulated by peptide assembly using fish viscera-derived peptides. According to encapsulation experiments, the optimal encapsulation settings were as follows: enzymatic hydrolysis time of 120 min, encapsulation time of 3 h, and the ideal zingerone to peptide ratio of 1:3 (*w*/w). The self-assembly of fish peptides effectively encapsulated zingerone in a stable state, as evidenced by the encapsulation structure visualized through CLSM and TEM. The uneven size and structure of the fish viscera peptide-zingerone complex can be attributed to variations in the molecular weight and surface hydrophobicity of fish peptides. In accordance with molecular interaction investigations, it was observed that zingerone and fish peptides interacted in a non-covalent manner. Furthermore, zingerone encapsulated by peptide assembly can significantly improve *in vitro* release of zingerone. In addition, *in vitro* inhibitory activities of fish viscera peptide-zingerone complex in Caco-2 cells were remarkably elevated mainly due to the peptide self-assembly encapsulation system. The present study can provide a theoretical basis for the application of peptides derived from fish viscera in the encapsulation of zingerone *via* peptide assembly. However, further study is still needed to understand the exact mechanism responsible for the anti-proliferative activity of the fish viscera peptide-zingerone complex.

Ethical approval

The present paper does not contain any human or animal studies.

CRediT authorship contribution statement

Sirong Huang: Writing – original draft, Validation, Methodology, Investigation. **Xintong Yao:** Writing – original draft, Validation, Investigation. **Boya Cao:** Validation, Investigation. **Na Zhang:** Writing – review & editing. **Olugbenga P. Soladoye:** Writing – review & editing. **Yuhao Zhang:** Writing – review & editing, Resources. **Yu Fu:** Supervision, Funding acquisition, Conceptualization.

Declaration of competing interest

The authors declare that they have no known competing financial interests or personal relationships that could have appeared to influence the work reported in this paper.

Data availability

Data will be made available on request.

Acknowledgments

This study was funded by National Natural Science Foundation of China (32101980), Natural Science Foundation of Chongqing (CSTB2023NSCQ-MSX0304), Innovation Program for Chongqing's Overseas Returnees (cx2019072) and Innovation Training Program for College Students at Southwest University (S202310635352).

Appendix A. Supplementary data

Supplementary data to this article can be found online at https://doi.org/10.1016/j.fochx.2024.101506.

References

Akbari, A., & Wu, J. (2016). Cruciferin nanoparticles: Preparation, characterization and their potential application in delivery of bioactive compounds. *Food Hydrocolloids, 54*, 107–118.

Amin, I., Hussain, I., Rehman, M. U., Mir, B. A., Ganaie, S. A., Ahmad, S. B., … Ahmad, P. (2021). Zingerone prevents lead-induced toxicity in liver and kidney tissues by regulating the oxidative damage in Wistar rats. *Journal of Food Biochemistry, 45*(3), Article e13241. https://doi.org/10.1111/jfbc.13241

Cao, S., Li, H., Zhao, Z., Zhang, S., Chen, J., Xu, J., … Brand, L. (2021). Ultrafast fluorescence spectroscopy via upconversion and its applications in biophysics. *Molecules, 26*(1), 211.

Chen, H., Cai, X., Cheng, J., & Wang, S. (2022). Self-assembling peptides: Molecule-nanostructure-function and application on food industry. *Trends in Food Science & Technology, 120*, 212–222. https://doi.org/10.1016/j.tifs.2021.12.027

Chen, H., Chen, X., Chen, X., Lin, S., Cheng, J., You, L., … Wang, S. (2022). New perspectives on fabrication of peptide-based nanomaterials in food industry: A review. *Trends in Food Science & Technology, 129*, 49–60. https://doi.org/10.1016/j.tifs.2022.09.004

Chen, M., Li, R., Gao, Y., Zheng, Y., Liao, L., Cao, Y., … Zhou, W. (2021). Encapsulation of hydrophobic and low-soluble polyphenols into nanoliposomes by pH-driven method: Naringenin and naringin as model compounds. *Foods, 10*(5), 963. https://www.mdpi.com/2304-8158/10/5/963

Dias, R., Bras, N. F., Perez-Gregorio, M., Fernandes, I., Mateus, N., & Freitas, V. (2019). A multi-spectroscopic study on the interaction of food polyphenols with a bioactive gluten peptide: From chemistry to biological implications. *Food Chemistry, 299*, 125051.

Du, Y., Bao, C., Huang, J., Jiang, P., Jiao, L., Ren, F., & Li, Y. (2019). Improved stability, epithelial permeability and cellular antioxidant activity of β-carotene via encapsulation by self-assembled α-lactalbumin micelles. *Food Chemistry, 271*, 707–714.

Elshopakey, G. E., Almeer, R., Alfaraj, S., Albasher, G., Abdelgawad, M. E., Abdel Moneim, A. E., & Essawy, E. A. (2022). Zingerone mitigates inflammation, apoptosis and oxidative injuries associated with renal impairment in adriamycin-intoxicated mice. *Toxin Reviews, 41*(3), 731–742. https://doi.org/10.1080/15569543.2021.1923528

Fu, Y., Liu, J., Hansen, E. T., Bredie, W. L., & Lametsch, R. (2018). Structural characteristics of low bitter and high umami protein hydrolysates prepared from bovine muscle and porcine plasma. *Food Chemistry, 257*, 163–171.

Fu, Y., Liu, J., Zhang, W., Wæhrens, S. S., Tøstesen, M., Hansen, E. T., … Lametsch, R. (2020). Exopeptidase treatment combined with Maillard reaction modification of protein hydrolysates derived from porcine muscle and plasma: Structure–taste relationship. *Food Chemistry, 306*, Article 125613.

Fu, Y., Liu, W., & Soladoye, O. P. (2021). Towards innovative food processing of flavonoid compounds: Insights into stability and bioactivity. *LWT, 111968*.

Fu, Y., & Zhao, X. H. (2015). Utilization of chum salmon (Oncorhynchus keta) skin gelatin hydrolysates to attenuate hydrogen peroxide-induced oxidative injury in rat

hepatocyte BRL cell model. *Journal of Aquatic Food Product Technology, 24*(7), 648–660.

Gao, Y., Lu, Y., Zhang, N., Udenigwe, C. C., Zhang, Y., & Fu, Y. (2022). Preparation, pungency and bioactivity of gingerols from ginger (Zingiber officinale roscoe): A review. *Critical Reviews in Food Science and Nutrition*, 1–26. https://doi.org/10.1080/10408398.2022.2124951

Ge, Z., Wang, Q., Zhu, Q., Yusif, M., Yu, J., & Xu, X. (2021). Improved oral bioavailability, cellular uptake, and cytotoxic activity of zingerone via nano-micelles drug delivery system. *Journal of Microencapsulation, 38*(6), 394–404. https://doi.org/10.1080/02652048.2021.1957036

Ketnawa, S., Benjakul, S., Martínez-Alvarez, O., & Rawdkuen, S. (2017). Fish skin gelatin hydrolysates produced by visceral peptidase and bovine trypsin: Bioactivity and stability. *Food Chemistry, 215*, 383–390.

Kieler-Ferguson, H. M., Chan, D., Sockolosky, J., Finney, L., Maxey, E., Vogt, S., & Szoka, F. C., Jr. (2017). Encapsulation, controlled release, and antitumor efficacy of cisplatin delivered in liposomes composed of sterol-modified phospholipids. *European Journal of Pharmaceutical Sciences, 103*, 85–93.

Kim, W., Thévenot, J., Ibarboure, E., Lecommandoux, S., & Chaikof, E. L. (2010). Self-assembly of thermally responsive amphiphilic diblock copolypeptides into spherical micellar nanoparticles. *Angewandte Chemie, 122*(25), 4353–4356.

Lan, M., Fu, Y., Dai, H., Ma, L., Yu, Y., Zhu, H., … Zhang, Y. (2021). Encapsulation of β-carotene by self-assembly of rapeseed meal-derived peptides: Factor optimization and structural characterization. *LWT, 138*, Article 110456.

Li, L., & Yao, P. (2020). High dispersity, stability and bioaccessibility of curcumin by assembling with deamidated zein peptide. *Food Chemistry, 319*, Article 126577. https://doi.org/10.1016/j.foodchem.2020.126577

Li, T., Lu, X. M., Zhang, M. R., Hu, K., & Li, Z. (2022). Peptide-based nanomaterials: Self-assembly, properties and applications. *Bioactive Materials, 11*, 268–282.

Liu, W., Wang, J., McClements, D. J., & Zou, L. (2018). Encapsulation of β-carotene-loaded oil droplets in caseinate/alginate microparticles: Enhancement of carotenoid stability and bioaccessibility. *Journal of Functional Foods, 40*, 527–535. https://doi.org/10.1016/j.jff.2017.11.046

Luo, J., Yao, X., Soladoye, O. P., Zhang, Y., & Fu, Y. (2021). Phosphorylation modification of collagen peptides from fish bone enhances their calcium-chelating and antioxidant activity. *LWT, 115*, Article 112978.

Ma, C. M., & Zhao, X. H. (2019). Depicting the non-covalent interaction of whey proteins with galangin or genistein using the multi-spectroscopic techniques and molecular docking. *Foods, 8*(9), 360.

Rashid, S., Wali, A. F., Rashid, S. M., Alsaffar, R. M., Ahmad, A., Jan, B. L., … Rehman, M. U. (2021). Zingerone targets status epilepticus by blocking hippocampal neurodegeneration via regulation of redox imbalance, inflammation and apoptosis. *Pharmaceuticals, 14*(2), 146. https://doi.org/10.3390/ph14020146

Rudke, A. R., Mazzutti, S., Andrade, K. S., Vitali, L., & Ferreira, S. R. S. (2019). Optimization of green PLE method applied for the recovery of antioxidant compounds from buriti (Mauritia flexuosa L.) shell. *Food Chemistry, 298*, 125061.

Shishir, M. R. I., Xie, L., Sun, C., Zheng, X., & Chen, W. (2018). Advances in micro and nano-encapsulation of bioactive compounds using biopolymer and lipid-based transporters. *Trends in Food Science & Technology, 78*, 34–60.

Sotelo-Boyás, M. E., Correa-Pacheco, Z. N., Bautista-Baños, S., & Corona-Rangel, M. L. (2017). Physicochemical characterization of chitosan nanoparticles and nanocapsules incorporated with lime essential oil and their antibacterial activity against food-borne pathogens. *LWT, 77*, 15–20. https://doi.org/10.1016/j.lwt.2016.11.022

Su, P., Veeraraghavan, V. P., Krishna Mohan, S., & Lu, W. (2019). A ginger derivative, zingerone—a phenolic compound—induces ROS-mediated apoptosis in colon cancer cells (HCT-116). *Journal of biochemical and molecular toxicology, 33*(12), Article e22403.

Vahedifar, A., & Wu, J. (2022). Self-assembling peptides: Structure, function, in silico prediction and applications. *Trends in Food Science & Technology, 119*, 476–494. https://doi.org/10.1016/j.tifs.2021.11.020

Villamil, O., Váquiro, H., & Solanilla, J. F. (2017). Fish viscera protein hydrolysates: Production, potential applications and functional and bioactive properties. *Food Chemistry, 224*, 160–171.

Wali, A. F., Rehman, M. U., Raish, M., Kazi, M., Rao, P. G., Alnemer, O., … Ahmad, A. (2020). Zingerone [4-(3-methoxy-4-hydroxyphenyl)-butan-2] attenuates lipopolysaccharide-induced inflammation and protects rats from sepsis associated multi organ damage. *Molecules, 25*(21), 5127. https://doi.org/10.3390/molecules25215127

Wang, Q., Huang, C.-R., Jiang, M., Zhu, Y.-Y., Wang, J., Chen, J., & Shi, J.-H. (2016). Binding interaction of atorvastatin with bovine serum albumin: Spectroscopic methods and molecular docking. *Spectrochimica Acta Part A: Molecular and Biomolecular Spectroscopy, 156*, 155–163. https://doi.org/10.1016/j.saa.2015.12.003

Wu, D., Duan, R., Tang, L., Hu, X., Geng, F., Sun, Q., … Li, H. (2021). Binding mechanism and functional evaluation of quercetin 3-rhamnoside on lipase. *Food Chemistry, 359*, 129960.

Yang, M., Liu, J., Li, Y., Yang, Q., Liu, C., Liu, X., … Du, Z. (2022). Co-encapsulation of egg-white-derived peptides (EWDP) and curcumin within the polysaccharide-based amphiphilic nanoparticles for promising Oral bioavailability enhancement: Role of EWDP. *Journal of Agricultural and Food Chemistry, 70*(16), 5126–5136. https://doi.org/10.1021/acs.jafc.1c08186

Yin, J., Huang, L., Wu, L., Li, J., James, T. D., & Lin, W. (2021). Small molecule based fluorescent chemosensors for imaging the microenvironment within specific cellular regions. *Chemical Society Reviews, 50*(21), 12098–12150.

Yu, M., Lin, S., Ge, R., Xiong, C., Xu, L., Zhao, M., & Fan, J. (2022). Buckwheat self-assembling peptide-based hydrogel: Preparation, characteristics and forming mechanism. *Food Hydrocolloids, 125*, Article 107378.

Yu, M., Yuan, W., Li, D., Schwendeman, A., & Schwendeman, S. P. (2019). Predicting drug release kinetics from nanocarriers inside dialysis bags. *Journal of Controlled Release, 315*, 23–30. https://doi.org/10.1016/j.jconrel.2019.09.016

Zhang, Y., Zhou, F., Zhao, M., Lin, L., Ning, Z., & Sun, B. (2018). Soy peptide nanoparticles by ultrasound-induced self-assembly of large peptide aggregates and their role on emulsion stability. *Food Hydrocolloids, 74*, 62–71. https://doi.org/10.1016/j.foodhyd.2017.07.021

Zhao, H., Guo, M., Ding, T., Ye, X., & Liu, D. (2020). Exploring the mechanism of hollow microcapsule formation by self-assembly of soy 11s protein upon heating. *Food Hydrocolloids, 108*, 105379.

Zhao, Y., Yang, W., Chen, C., Wang, J., Zhang, L., & Xu, H. (2018). Rational design and self-assembly of short amphiphilic peptides and applications. *Current Opinion in Colloid & Interface Science, 35*, 112–123. https://doi.org/10.1016/j.cocis.2018.02.009